49th AIAA/ASME/ASCE/AHS/ASC Structures, Structural Dynamics, and Materials Conference
 16t
7 - 10 April 2008, Schaumburg, IL

AIAA 2008-1896

Least-Squares Continuous Sensitivity Analysis of an Example Fluid-Structure Interaction Problem

Douglas P. Wickert[1], Robert A. Canfield[2]
Air Force Institute of Technology, Wright-Patterson AFB, OH, 45433, USA

A least-squares continuous sensitivity analysis method is developed for fluid-structure interaction problems to support computationally efficient analysis and optimization of aeroelastic design problems. The continuous sensitivity system equations and sensitivity boundary conditions are derived and the problem is posed in first-order form. A least-squares finite element solution of the fully-coupled fluid-structure physics is then used to determine the sensitivity boundary conditions. The least-squares finite element method permits a simultaneous solution of the fluid-structure system and the mesh deformation problem within a single numerical framework. A least-squares finite element solution of the linear continuous sensitivity equations is then used to produce computationally efficient design parameter gradient calculations without needing to calculate the problematic mesh sensitivities. An example fluid-structure interaction problem with a known analytic solution is solved. Continuous sensitivity results are presented and compared to closed-form analytic gradients.

I. Introduction

Ongoing research efforts are seeking new methods for effective and computationally efficient analysis of high-fidelity, nonlinear, aeroelastic models suitable for aircraft gust response [1]. Aeroelasticity is a challenging science, dealing with the interaction of two very different domains governed by disparate physics. Nonlinear aspects of both the fluid and structural domains can make accurate calculations of the interaction problematic, not the least due to the substantial computational expenses involved. Since optimization and inverse design methods typically require some measure of the change of an objective function or performance parameter to variations in design parameters, optimization of aeroelastic problems, which are themselves computationally intensive, challenging, and expensive to solve, can be outright formidable. Thus, this subject represents a very prime frontier for basic research

Currently, the most common approach for solving fluid-structure interaction (FSI) problems uses different theoretical formulations and numerical methods to solve the fluid and structure problems separately, a method that can be fraught with convergence issues and inaccurate solutions when the method does converge [2, 3]. A more significant drawback is that when applied to sensitivity applications, the iterative nature of the segregated strategy may require multiple computationally expensive cycles for every variation of an individual design variable. If scaled to hundreds or thousands of design variables, the segregated method is computationally intractable. Thus, although segregated methods are suitable for many design applications and have been used with success in multidisciplinary optimization, these loosely-coupled or weakly-coupled approaches are simply computationally inadequate for large-scale optimization of dynamic aeroelastic problems. An alternative FSI solution strategy casts the coupled fluid, structure, and mesh deformation systems as a single monolithic or fully-coupled fluid-structure-mesh formulation [4-6]. This approach generally gives the fastest convergence [7], though the memory requirements are substantially greater since the fluid, structure, and mesh degrees of freedom must be treated and

The views expressed in this paper are those of the author and do not reflect the official policy or position of the United States Air Force, Department of Defense, or the United States Government.

[1] PhD Student, Department of Aeronautical and Astronautical Engineering, 2950 Hobson Way, Wright-Patterson AFB, OH 45433-7765, AIAA Student Member.

[2] Associate Professor, Department of Aeronautical and Astronautical Engineering, 2950 Hobson Way, Wright-Patterson AFB, OH 45433-7765, AIAA Member Grade.

solved simultaneously. As overall computer performance improves and the expense of large memory approaches decreases, the trend in aeroelastic computational methods is towards full coupling of the fluid-structure-mesh systems [8, 9]. For design sensitivity calculations, a monolithic solution strategy is probably essential.

Design sensitivity methods can be grouped [10] into numerical approximate methods or analytic and semi-analytic methods as indicated in Figure 1 . Analytic and semi-analytic methods can be further classified as either discrete or continuous, the difference depending on the order of the discretization and differentiation steps [11]. The most common approach is to discretize the system first and calculate sensitivities by either direct or adjoint methods. For shape sensitivity problems, the mesh sensitivity must also be calculated which can be problematic. In continuous sensitivity analysis, the design parameter gradients are calculated from the continuous equations yielding a system of differential equations for the sensitivity variables, which are, in turn, discretized [12, 13]. Thus, the continuous sensitivity method for gradient calculation can efficiently produce design parameter gradients needed by most optimization algorithms without needing to invert the mesh Jacobian. The resulting sensitivity system of equations is always linear, even for nonlinear systems, which is particularly attractive for the nonlinear aeroelastic problems considered here.

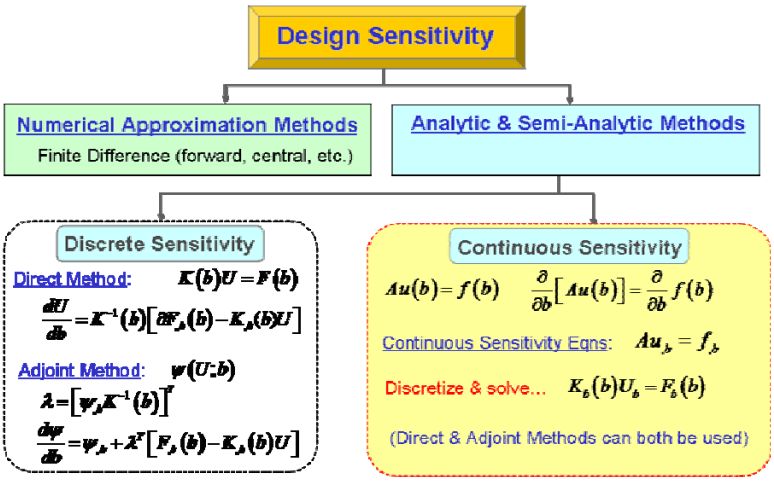

Figure 1 Classification and methods of design sensitivity analysis

Overall, shape sensitivity and optimization methods are more mature for structural problems [14] than they are for fluid problems, but they have not typically employed continuous sensitivity methods [11, 15]. Although there now exists an extensive body of literature involving the application of continuous sensitivity methods to fluid dynamics problems, the application to structural elasticity problems is complicated by the nature of the sensitivity of the stress tensor [16, 17]. Shape sensitivity methods have been applied to fluid-structure interaction problems in several studies[18], but the use of continuous sensitivity methods in aeroelasticity is far more limited and recent [19][20][21]. To our knowledge, this is the first effort to use least-squares finite element (LSFEM) methods to solve both the fully-coupled fluid-structure interaction physics and the sensitivity equations with the same computational framework.

A LSFEM formulation for the FSI problem is promising in that it provides a consistent approach with the same numerical framework for the simultaneous solution of the fully-coupled fluid, structure , and accompanying mesh deformation problems [22][23]. The LSFEM method is in the class of weighted residual variational solutions to partial differential equations and has seen a renaissance of interest in the last several years: [23-32] are representative of the range of applications to both fluid and structural problems. A LSFEM approach seeks to minimize the L^2 norm of the residual error of the governing differential equations. Least-squares methods for time-dependent and nonlinear problems are well-established in the literature [25], and appear applicable to analysis of transient, nonlinear gust response. Gust response loads are of particular interest as they have been identified as the critical load condition for several proposed aerospace applications, including a next-generation, long-endurance vehicle designed for persistent intelligence, surveillance, and reconnaissance missions [33, 34]. The sensitivity to transient gust loads will be considered in future work.

This paper begins with a description of the fully-coupled fluid, structure, and interface system of equations and the formulation of the least-squares finite element solution. Then the continuous sensitivity system of equations and the sensitivity boundary conditions are derived. The next section details the LSFEM computational approach used

to solve the sensitivity equations. Finally, design parameter sensitivities in an example FSI problem with a known analytic solution are solved using the least-squares continuous sensitivity method. The continuous sensitivity results are presented and compared to closed-form approximate-analytic gradients.

II. Monolithic Fluid-Structure-Mesh Coupling and Interface Conditions

In the monolithic approach, the structure, fluid, and mesh deformation are fully-coupled and posed as a single, implicit system [4]. Some researchers have employed different finite element formulations for each domain. For example [35] uses LSFEM for the fluid solution and a weak-Galerkin FEM for the structure solution. In the present effort, we use a unified, higher-order p LSFEM formulation for the structure, fluid, and mesh deformation domains. Thus, the fully-coupled structure-fluid-mesh system takes the form

$$\begin{bmatrix} \left[K^{ss}\right] & \left[K^{sf}\right] & \left[K^{sd}\right] \\ \left[K^{fs}\right] & \left[K^{ff}\right] & \left[K^{fd}\right] \\ \left[K^{ds}\right] & \left[K^{df}\right] & \left[K^{dd}\right] \end{bmatrix} \begin{Bmatrix} U^s \\ U^f \\ U^d \end{Bmatrix} = \begin{Bmatrix} F^s \\ F^f \\ F^d \end{Bmatrix} \tag{1}$$

where s denotes the structure domain, f the fluid domain, and d denotes the deformation domain.

The interface conditions on the fluid structure boundary, Γ^{sf}, are based on kinematic and equilibrium conditions along the interface between the structure and fluid domains. If the outward normal vectors for the structure and fluid domains are $\mathbf{n}^s$ and $\mathbf{n}^f$, then $\mathbf{n}^s = -\mathbf{n}^f$ on Γ^{sf}. For viscous flow, the no slip condition is

$$\mathbf{v}^s - \mathbf{v}^f = 0 \quad \text{on } \Gamma^{sf} \tag{2}$$

where $\mathbf{v}^s$ and $\mathbf{v}^f$ are the structure and fluid velocities respectively. For steady-state problems, the structure velocity is zero. Equilibrium conditions on the fluid-structure interface result in

$$\boldsymbol{\sigma}^s \cdot \mathbf{n}^s + \boldsymbol{\sigma}^f \cdot \mathbf{n}^f = 0 \quad \text{on } \Gamma^{sf} \tag{3}$$

which equates the structure boundary stress vector, $\boldsymbol{\sigma}^s \cdot \mathbf{n}^s$, to the traction forces due to the fluid stress at the interface, written in tensor index notation as

$$\sigma_{ij}^f = -p^f \delta_{ij} + \mu^f \left(u_{i,j}^f + u_{j,i}^f\right) + \delta_{ij} \lambda^f u_{i,i}^f \tag{4}$$

where μ^f is the fluid viscosity and λ^f is the fluid bulk viscosity. For the incompressible Stokes flow considered below, the fluid stress simplifies to

$$\sigma_{ij}^f = -p^f \delta_{ij} + \mu^f \left(u_{i,j}^f + u_{j,i}^f\right) \tag{5}$$

The interface coupling is incorporated into the LSFEM model by a boundary integral, (23), evaluated along Γ^{sf}. The LSFEM minimizes the fully-coupled weighted system residual

$$J_{tot} = \alpha^s J^s + \alpha^f J^f + \alpha^d J^d + \alpha^{sfd} J^{sfd} \tag{6}$$

where the α's are weighting factors and the structure, fluid, and mesh deformation system residuals (see Section III)

$$J^s\left(\Omega^s\right) = \left\| \mathbf{A}^s \mathbf{u}^s - \mathbf{f}^s \right\|_{L^2}^2 \tag{7}$$

$$J^f\left(\Omega^f\right) = \left\| \mathbf{A}^f \mathbf{u}^f - \mathbf{f}^f \right\|_{L^2}^2 \tag{8}$$

$$J^d\left(\Omega^d\right) = \left\| \mathbf{A}^d \mathbf{u}^d - \mathbf{f}^d \right\|_{L^2}^2 \tag{9}$$

L^2 norms are used to evaluate the domain residuals, however formal restriction of the domain function spaces to the boundary imply fractional dual space norms [36]. Since it is inconvenient to use the fractional norms, L^2 norms will be substituted in the boundary integral evaluation using the mesh-dependent weightings. Thus, the interface residual becomes

$$J^{sfd}\left(\Gamma^{sf}\right)=\alpha_1\frac{1}{\sqrt{h}}\left\|\mathbf{v}^s-\mathbf{v}^f\right\|_{L^2}^2+\alpha_2\sqrt{h}\left\|\boldsymbol{\sigma}^s\cdot\mathbf{n}^s+\boldsymbol{\sigma}^f\cdot\mathbf{n}^f\right\|_{L^2}^2+\alpha_3\left\|u^s-d^s\right\|_{L^2}^2 \tag{10}$$

The diagonal components of the stiffness matrix in (1) are constructed on an element basis and assembled into the global system by separate evaluation in each domain. The coupling components of (1) are determined from evaluating the boundary integral along the interface and assembling the boundary element degrees of freedom into the global system based on a global degree of freedom index table.

In the example problem presented in Section V, a flexible 1D Euler-Bernoulli beam divides two channels with pressure-driven Stokes flow. Different flow rates through the channels results in a differential pressure load and deflection of the beam. Though the Stokes equations are physically valid only for very low Reynolds numbers, they are useful for our present purpose of developing a continuous sensitivity least-squares method for FSI. The Stokes equations are a set of linear equations which permit straightforward solutions for developing FSI and CSE methods without the complexity of nonlinear terms which would contribute little further understanding. The next two sections detail the Stokes and Euler-Bernoulli differential systems.

A. Stokes Flow

In creeping flow, originally developed by Stokes c. 1851, the fluid inertial forces are considered negligible relative to the viscous forces $\left(Re\ll 1\right)$. Thus there are no acceleration terms in the momentum equation and it is only valid to consider steady state conditions. The Stokes equations in basic form are [37]

$$\begin{aligned}&-\mu\nabla^2\mathbf{u}+\nabla p=\mathbf{f}\quad\text{in }\Omega\\&\nabla\mathbf{u}=0\quad\text{in }\Omega\end{aligned} \tag{11}$$

where μ is viscosity, $\mathbf{u}$ is the fluid velocity vector, p is pressure, and $\mathbf{f}$ is the body force. To implement (11) using LSFEM, it is convenient to introduce vorticity, $\boldsymbol{\omega}\equiv\nabla\times\mathbf{u}$, and express (11) as a div-curl system [25]

$$\begin{aligned}&\nabla p+\mu\nabla\times\boldsymbol{\omega}=\mathbf{f}\quad\text{in }\Omega\\&\nabla\cdot\boldsymbol{\omega}=0\quad\text{in }\Omega\\&\boldsymbol{\omega}-\nabla\times\mathbf{u}=\mathbf{0}\quad\text{in }\Omega\\&\nabla\cdot\mathbf{u}=0\quad\text{in }\Omega\end{aligned} \tag{12}$$

which is now a first-order system and practical for LSFEM. In 2D ,vorticity, $\omega\equiv u_{,y}+v_{,x}$, is a scalar and (12) in component form is

$$\begin{aligned}&p_{,x}+\mu\omega_{,y}=f_x\quad\text{in }\Omega\\&p_{,y}-\mu\omega_{,x}=f_y\quad\text{in }\Omega\\&u_{,x}+v_{,y}=0\quad\text{in }\Omega\\&\omega+u_{,y}-v_{,x}=0\quad\text{in }\Omega\end{aligned} \tag{13}$$

which in matrix operator form with $\mathbf{u}^f=\left\{u\quad v\quad p\quad\omega\right\}^T$ is

$$A_0^f\mathbf{u}^f+A_1^f\mathbf{u}_{,x}^f+A_2^f\mathbf{u}_{,y}^f=\mathbf{f}^f \tag{14}$$

where

$$A_0^f=\begin{bmatrix}0&0&0&0\\0&0&0&0\\0&0&0&0\\0&0&0&1\end{bmatrix}\quad A_1^f=\begin{bmatrix}1&0&0&0\\0&0&1&0\\0&0&0&-\mu\\0&-1&0&0\end{bmatrix}\quad A_2^f=\begin{bmatrix}0&1&0&0\\0&0&0&\mu\\0&0&1&0\\1&0&0&0\end{bmatrix}\quad \mathbf{f}^f=\begin{bmatrix}0\\f_x\\f_y\\0\end{bmatrix} \tag{15}$$

The *f* superscripts are introduced to denote fluid domain variables.

The appropriate boundary conditions combinations for (12) are either 1) p and $\mathbf{n}\cdot\boldsymbol{\omega}$ or 2) $\mathbf{n}\times\boldsymbol{\omega}$ (see [25] 8.2.2). For 2D, these two set of boundary conditions reduce to the combinations given in Table 1 .

Table 1 : Boundary condition combinations for the Stokes equations (from [25])

Description	Boundary Condition
Inlet	$\mathbf{n}\cdot\mathbf{u}$ and ω
Inlet	$\mathbf{n}\cdot\mathbf{u}$ and p
Outlet	$\mathbf{n}\times\mathbf{u}$ and p
Uniform outflow	$\mathbf{n}\times\mathbf{u}$ and ω
Wall	$\mathbf{n}\times\mathbf{u}$ and $\mathbf{n}\cdot\mathbf{u}$
Outlet (portion of Γonly)	p and ω

B. Euler-Bernoulli Beam

The governing equation for the deflection, v, of an Euler-Bernoulli beam subject to a transverse load per unit length, p_y is [38]

$$\rho\frac{\partial^2 v}{\partial t^2}+\frac{\partial^2}{\partial x^2}\left(EI\frac{\partial^2 v}{\partial x^2}\right)=p_y \tag{16}$$

Introducing

$$\theta = v_{,x} \tag{17}$$

$$M_z = EIv_{,xx} = \theta_{,x} \tag{18}$$

$$V_y = -M_{z,x} \tag{19}$$

where θ is the beam slope, M_z is the internal bending moment, and V_y is the internal shear force allows decomposition of (16) into first-order form.

$$A_t^s\mathbf{u}_{,tt}^s + A_0^s\mathbf{u}^s + A_1^s\mathbf{u}_{,x}^s = \mathbf{f}^s \tag{20}$$

where $\mathbf{u}^s = \begin{bmatrix} v & \theta & M_z & V_y \end{bmatrix}^T$ and the matrix operators are

$$A_t^s=\begin{bmatrix}0&0&0&0\\0&0&0&0\\0&0&0&0\\\rho^s&0&0&0\end{bmatrix}\quad A_0^s=\begin{bmatrix}0&1&0&0\\0&0&1/EI&0\\0&0&0&-1\\0&0&0&0\end{bmatrix}\quad A_1^s=\begin{bmatrix}-1&0&0&0\\0&-1&0&0\\0&0&-1&0\\0&0&0&-1\end{bmatrix}\quad \mathbf{f}^s=\begin{bmatrix}0\\0\\0\\p_y\end{bmatrix} \tag{21}$$

C. Mesh Deformation Domain

To permit a monolithic formulation of CSE FSI system including the moving fluid mesh, the fluid domain mesh deformation must be modeled as a continuum. This precludes the commonly used discrete method of connecting springs between grid points to move the domain. The mesh domain can be treated as continuous elastic solid, a pseudo-solid, a technique first introduced in [39] and successfully applied to FSI sensitivity calculations by [5]. For our present goal of developing and understanding the details a continuous sensitivity least-square method for FSI, we consider small deflections of the structure obviating the need for a mesh deformation solution which will be included in future work.

III. Least-Squares Finite Element Method

Consider the following general boundary value system defined in a domain Ω with a boundary Γ for which we seek a solution $\mathbf{u}$

$$\mathbf{Au} = \mathbf{f} \text{ in } \Omega \tag{22}$$
$$\mathbf{Bu} = \mathbf{g} \text{ on } \Gamma \tag{23}$$

A is a first-order time-space differential operator given by

$$\mathbf{A} = \mathbf{A}_t \frac{\partial}{\partial t} + \sum_{i=1}^{\dim} \mathbf{A_i} \frac{\partial}{\partial x_i} + \mathbf{A_0} \tag{24}$$

B, the boundary condition operator, has the form

$$\mathbf{B} = \mathbf{B}_t \frac{\partial}{\partial t} + \mathbf{B}_1 \frac{\partial}{\partial \xi_i} + \mathbf{B_0} \tag{25}$$

where ξ is a coordinate that parametizes the boundary (e.g. arc length). The square of the system weighted residuals defines a functional (c.f. (6) thru (9))

$$J(\mathbf{u};\mathbf{f},\mathbf{g}) = \alpha \left\| \mathbf{Au - f} \right\|_\Omega^2 + (1-\alpha) \left\| \mathbf{Bu - g} \right\|_\Gamma^2 \tag{26}$$

where

$$\left\| \cdot \right\|_\Omega^2 \equiv \int_\Omega (\cdot)^2 d\Omega \geq 0 \quad \text{and} \quad \left\| \cdot \right\|_\Gamma^2 \equiv \int_\Gamma (\cdot)^2 d\Gamma \geq 0 \tag{27}$$

are the L^2 norms and $0 < \alpha < 1$ are residual weighting factors. A necessary condition for **u** to minimize (26) is that the first variation of (26) vanishes at **u** [40]. This yields an equivalent bilinear/linear inner product form [41] for the boundary value system (22)-(23)

$$B(\mathbf{u},\mathbf{v}) = l(\mathbf{f},\mathbf{v}) \quad \forall \mathbf{v} \in \mathbf{V} \tag{28}$$

where

$$\begin{aligned} B_\Omega(\mathbf{u},\mathbf{v}) &\equiv (\mathbf{Au},\mathbf{Av}) \\ l_\Omega(\mathbf{f},\mathbf{v}) &\equiv (\mathbf{f},\mathbf{Av}) \end{aligned} \tag{29}$$

and

$$\begin{aligned} B_\Gamma(\mathbf{u},\mathbf{v}) &\equiv (\mathbf{Bu},\mathbf{Bv}) \\ l_\Gamma(\mathbf{g},\mathbf{v}) &\equiv (\mathbf{g},\mathbf{Bv}) \end{aligned} \tag{30}$$

For most of our present effort, $\mathbf{V} \subseteq L_2(\Omega)$, the *Lebesque* space consisting of square-integrable functions; or $\mathbf{V} \subseteq H^1(\Omega)$, the basic *Sobolev* space (a *Hilbert* space with first-order derivatives defined) [42]. The domain will be partitioned into finite elements and in each element, we approximate the solution **u** by

$$\mathbf{u} \approx \mathbf{u}_h^e = \sum_{j=1}^{n_{dof}^e} \psi_j \left[u_1 \ldots u_{n_{nodes}} \quad a_1 \ldots a_{n_a} \quad b_1 \ldots b_{n_a} \right]^T \tag{31}$$

where ψ_j are shape functions [43]. The element degrees of freedom, $n_{dof}^e = n_{nodes} + n_a + n_b$, consist of the element nodal values, $u_1 \ldots u_{n_{nodes}}$, the edge coefficients, $a_1 \ldots a_{n_a}$, and the interior (bubble) mode coefficients, $b_1 \ldots b_{n_a}$. This set of degrees of freedom assumes a higher-order hierarchal expansion of shape functions [44]. In what follows, we adopt Szabo's quadrilateral shape function expansion basis [45] which is a serendipity expansion built of kernel functions constructed from Legendre polynomials. Another commonly used expansion consisting of complete polynomials is based on a tensor product expansion of Legendre polynomials in two dimensions [46]. Note that different *p* values may be used to approximate each of the domains in (1).

Substituting (31) into (29) yields n^e_{dof} algebraic equations which are evaluated to determine the element stiffness matrix and equivalent force vector

$$\mathbf{K}^e = \int_{\Omega^e} \left(\mathbf{A}\psi_1, ..., \mathbf{A}\psi_{n^e_{dof}} \right)^T \left(\mathbf{A}\psi_1, ..., \mathbf{A}\psi_{n^e_{dof}} \right) d\Omega \tag{32}$$

$$\mathbf{F}^e = \int_{\Omega^e} \left(\mathbf{A}\psi_1, ..., \mathbf{A}\psi_{n^e_{dof}} \right)^T \mathbf{f} \; d\Omega \tag{33}$$

$$\mathbf{K}^e_\Gamma = \int_{\Gamma^e} \left(\mathbf{B}\psi_1, ..., \mathbf{B}\psi_{n^e_{dof}} \right)^T \left(\mathbf{B}\psi_1, ..., \mathbf{B}\psi_{n^e_{dof}} \right) d\Gamma \tag{34}$$

$$\mathbf{G}^e = \int_{\Gamma^e} \left(\mathbf{B}\psi_1, ..., \mathbf{B}\psi_{n^e_{dof}} \right)^T \mathbf{g} \; d\Gamma \tag{35}$$

The element stiffness and load vectors are assembled into a global system based on a global dof table. The global system then has the form

$$\left[\alpha \mathbf{K} + (1-\alpha) \mathbf{K}_\Gamma \right] \mathbf{u} = \alpha \mathbf{F} + (1-\alpha) \mathbf{G} \tag{36}$$

IV. Continuous Sensitivity Equations

The continuous sensitivity method differentiates the continuous system to yield a governing system of equations for the sensitivity variables. For example, differentiating some governing field equations with respect to a design parameter, *b*

$$\frac{\partial}{\partial b} \left[A_t \, \mathbf{u}_{,tt} + A_0 \mathbf{u} \; + A_1 \mathbf{u}_{,x} + A_2 \mathbf{u}_{,y} \right] = \frac{\partial}{\partial b} \left[\mathbf{f} \; \right] \tag{37}$$

$$A_t \, \frac{\partial}{\partial b} \frac{\partial^2 \mathbf{u}}{\partial t^2} + A_0 \, \frac{\partial}{\partial b} \mathbf{u} \; + A_1 \, \frac{\partial}{\partial b} \frac{\partial \mathbf{u}}{\partial x} + A_2^s \, \frac{\partial}{\partial b} \frac{\partial \mathbf{u}}{\partial y} = \frac{\partial \mathbf{f}}{\partial b} \tag{38}$$

$$A_t \left({}^b\mathbf{u}_{,tt} \right) + A_0 \left({}^b\mathbf{u} \; \right) + A_1 \left({}^b\mathbf{u}_{,x} \right) + A_2 \left({}^b\mathbf{u}_{,y} \right) = 0 \tag{39}$$

Since the spatial-temporal derivatives are independent operations from the sensitivity derivative, the order of differentiation may be reversed. Now, for example, defining the E-B Beam structure sensitivity variables as

$${}^b\mathbf{u}^s \equiv \frac{\partial}{\partial b} \mathbf{u}^s = \left[v^s_{,b} \quad \theta^s_{,b} \quad M^s_{z,b} \quad V^s_{y,b} \right]^T \tag{40}$$

yields the final CSE system

$$A^s_t \left({}^b\mathbf{u}^s_{,t} \right) + A^s_0 \left({}^b\mathbf{u}^s \right) + A^s_1 \left({}^b\mathbf{u}^s_{,x} \right) + A^s_2 \left({}^b\mathbf{u}^s_{,y} \right) = 0 \tag{41}$$

The CSE may now be discretized and solved using the same LSFEM method used to solve the FSI system. The continuous sensitivity system is thus simply another system of differential equations which together with the appropriate boundary data represents a well-conditioned boundary value problem which may be solved by any of a wide variety of numerical approaches. It is convenient in many cases to use the same numerical method/framework to solve the sensitivity system as was used to solve the original system.

The sensitivity equation boundary conditions specify how the sensitivity variables behave on the boundary of the domain. For shape variation problems, there are two ways in which boundary values for a scalar or vector field variable (considered component-wise), *u*, may change on the boundary. First, the boundary condition of the original problem may be altered by a change in the design parameter. Second, the design parameter may alter the shape of the boundary and domain and thus the value of the field variable. These are related through the concept of the material derivative

$$\left.\frac{Du}{Db}\right|_{\mathbf{X}} = \left.\frac{\partial u}{\partial b}\right|_{\mathbf{x}} + \nabla u \cdot \left.\frac{\partial \mathbf{x}}{\partial b}\right|_{\mathbf{X}} \tag{42}$$

where **X** denotes a material coordinate and **x** denotes a spatial coordinate (Eulerian description). Thus the total derivative of u with respect to b at a material point $\mathbf{X}_0$ consists of the local derivative of u with respect to parameter b and a transport term which accounts for how the material point $\mathbf{X}_0$ changes character in spatial coordinates as the design parameter b varies. (The transport of a scalar quantity in a vector field is most properly classified as advection, though convection is commonly used to refer to the second expression on the right hand side of (42). Most accurately, convection is the sum of advective transport and diffusive transport.) If u is a vector quantity, then the gradient operation and dot product in the advection term is carried out row-wise. The desired sensitivity variable boundary condition for a scalar or vector quantity is thus

$${}^{b}\mathbf{u}\big|_{\Gamma} \equiv \left.\frac{\partial \mathbf{u}}{\partial b}\right|_{\mathbf{X}=\Gamma} = \left.\frac{D\mathbf{u}}{Db}\right|_{\Gamma} - \nabla \mathbf{u} \cdot \frac{\partial \mathbf{x}_{\Gamma(b)}}{\partial b} \tag{43}$$

The first term on the right hand side accounts for how the boundary conditions for the problem change with respect to the design parameter. In most cases, this term is zero. That is, the boundary condition does not change as the shape changes. The advection term uses the gradient of the solution. In a finite element solution, this expression comes from the gradient of the shape functions applied to the finite element solution.

If the dependent variable is a tensor, as in the case of the fluid or structure stress tensor, then the more complicated upper convected derivative or Oldroyd derivative must be used in place of (42)

$$\mathbf{S}^{\nabla} = \frac{D}{Db}\mathbf{S} - \left(\nabla \frac{\partial \mathbf{x}}{\partial b}\right)^{T} \cdot \mathbf{S} - \mathbf{S} \cdot \left(\nabla \frac{\partial \mathbf{x}}{\partial b}\right) \tag{44}$$

where $\nabla \partial \mathbf{x}/\partial b$ is the tensor of design parameter velocities. (44) is equivalent to the stress tensor sensitivity expressed in terms normal and tangential surface tractions derived in a much different manner by Dems and Haftka [16]

$${}^{b}\sigma_{ij}^{s} n_j = \frac{DT_i}{Db} - \sigma_{ij,k} n_j \frac{\partial \phi_k}{\partial b} - \sigma_{ij}\left(n_j n_l - \delta_{jl}\right) n_k \left[\frac{\partial \phi_k}{\partial b}\right]_{,l} \tag{45}$$

where tensor index notation has been used, T_i are the components of the surface traction vector, n_i are the components of the unit normal/tangential vector, δ is the delta function, and ϕ is the transformation field that maps material coordinates of the domain as a function of the design parameter. Comparison and expansion of (44) and (45) is considered in a companion work [47].

V. FSI and CSE Example Problem

The example FSI problem in Figure 1 has a closed-form analytic solution [48]. A flexible 1D Euler-Bernoulli beam divides two channels with pressure-driven Stokes flow. Different flow rates through the channels results in a differential pressure load and deflection of the beam.

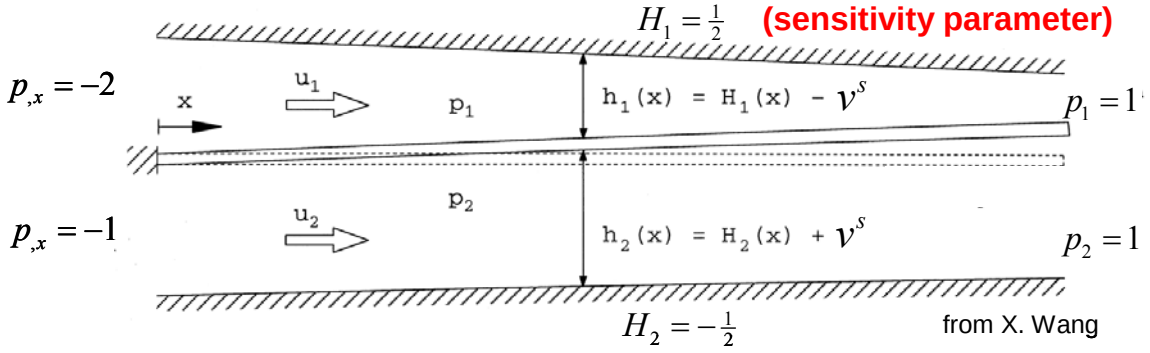

Figure 2 Beam immersed in a channel flow (X. Wang)

The FSI problem boundary conditions are given in Table 2 For our present goal of developing and understanding the details of a continuous sensitivity least-square method for FSI, we consider small deflections of the structure only, obviating the need for a mesh deformation solution. Thus, the mesh deformation is decoupled from the FSI system and CSE system. The slip wall boundary condition

$$\begin{aligned} u_t &= u^f \cos\theta^s + v^f \sin\theta^s = 0 \\ u_n &= -u^f \sin\theta^s + v^f \cos\theta^s = 0 \end{aligned} \tag{46}$$

results in a nonlinear coupling term through the boundary integral evaluation of (34) requiring an iterative solution. In the results presented below, due to the small deflections and linear fluid and structure equations, the solution converges in a single iteration. The LSFEM FSI solution is given in Figure 3 and the beam deflection is compared to the analytic solution [48] in Figure 4 .

Table 2 Beam in channel flow boundary conditions

Boundary	Constrained dofs	
inlet	$u = \frac{-1}{2\mu}\left(yh - y^2\right) p_{,x}$; $\omega = -u_{,y}$	fully-developed Poiseuille flow
outlet	$v = 0 \quad p = 1$	uniform outflow
walls	$u_t = u^f \cos\theta^s + v^f \sin\theta^s = 0$ $u_n = -u^f \sin\theta^s + v^f \cos\theta^s = 0$	no slip wall
beam-fluid interface	$V^s_{y,x} + \left(p^f_1 - p^f_2\right) = 0$	force equilibrium
mesh	$\mathbf{d}_i = \left(0 \quad w\frac{1}{h_i}\left[h_i - y\right]\right)$	vertically scaled deformation (de-coupled from fs solution)

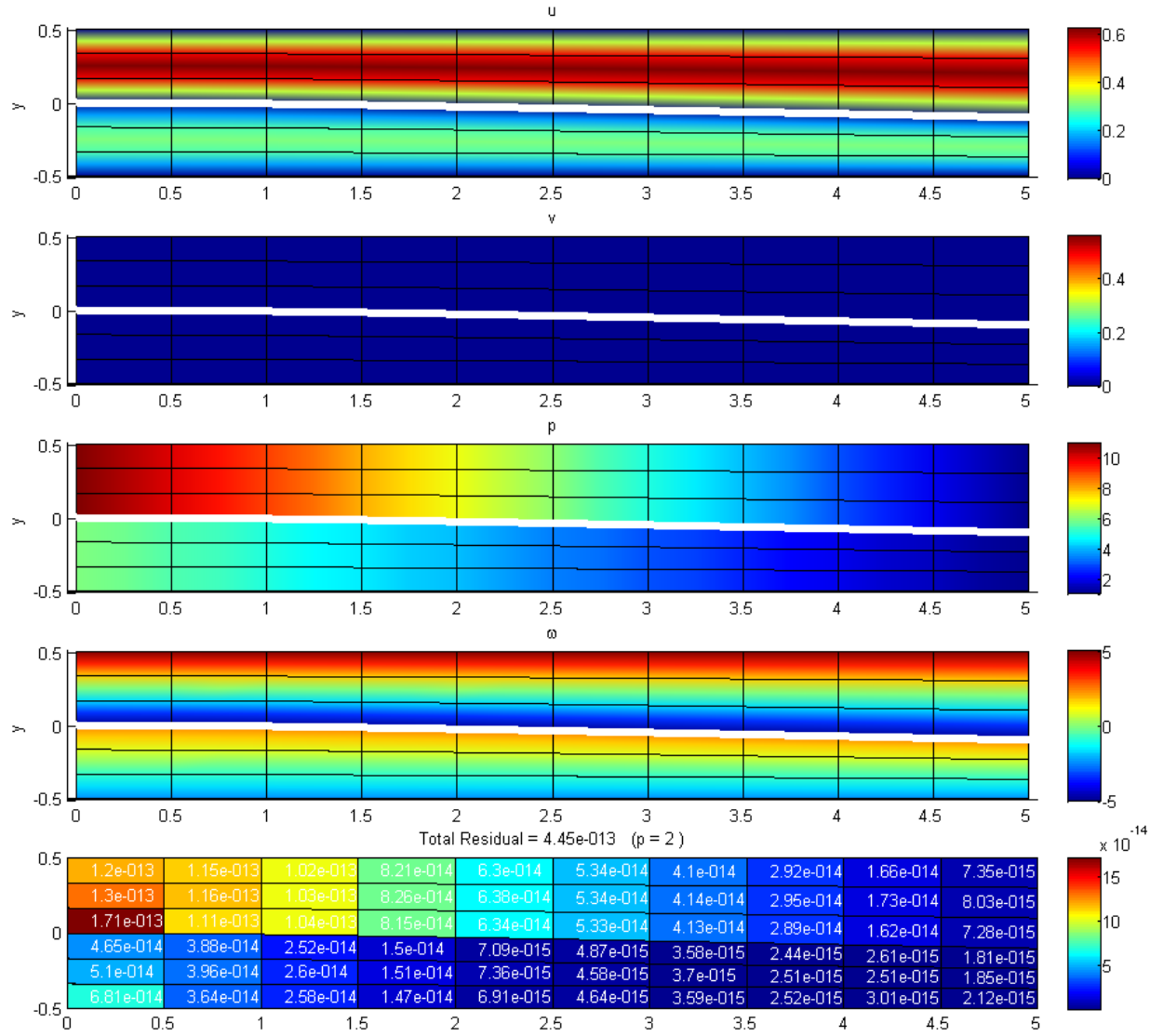

Figure 3 LSFEM FSI solution ($p = 2$) showing beam deflection

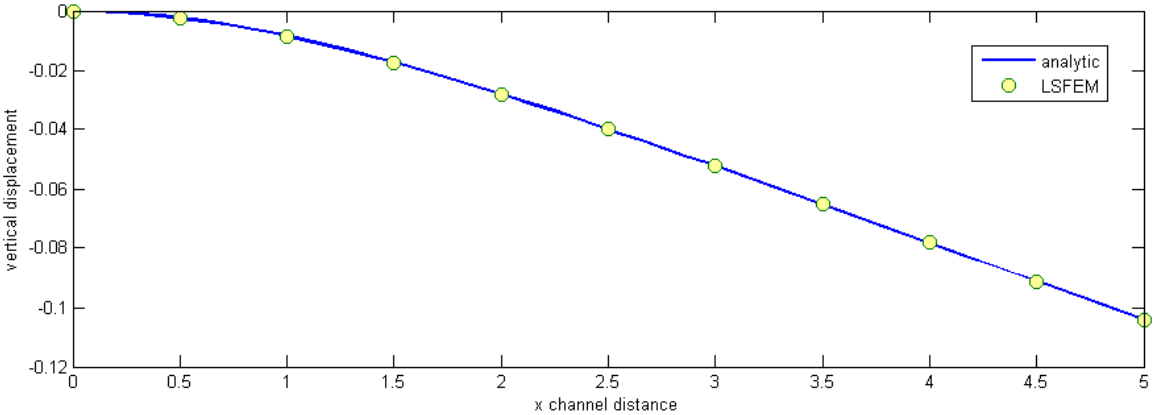

Figure 4 LSFEM and analytic solution for beam deflection

The solution gradients required for the CSE boundary conditions are determined by taking derivatives of the shape functions. Taking the upper channel height as the shape design parameter, we compute the sensitivity of the fluid domain flow and the beam deflection (given the same flow rate through the upper channel as the height changes) to the upper channel height. The upper channel wall is parameterized as the Cartesian ordered pair

$$X_{\Gamma_1^{top}} = \left\{ \begin{pmatrix} \xi & H_1 \end{pmatrix} \middle| \, \xi \in [0, L] \right\} \tag{47}$$

where L is the length of the channel. Then

$$\frac{\partial}{\partial H_1} X_{\Gamma_1^{top}} = \left\{ \begin{pmatrix} 0 & 1 \end{pmatrix} \right\} \tag{48}$$

Since the upper wall remains a no slip wall with variations in H_1, the upper wall CSE boundary condition reduces to

$$\begin{Bmatrix} {}^{H}u^f \\ {}^{H}v^f \end{Bmatrix} = 0 - \begin{Bmatrix} \nabla u^f \\ \nabla v^f \end{Bmatrix} \cdot \frac{\partial X_{\Gamma_1^{top}}}{\partial H_1} = \begin{Bmatrix} -u^f_{,y} \\ -v^f_{,y} \end{Bmatrix} \tag{49}$$

Similarly, parameterizing the upper inlet by

$$X_{\Gamma_1^{inlet}} = \left\{ \begin{pmatrix} 0 & 2\xi H_1 \end{pmatrix} \middle| \, \xi = y \in [0, \tfrac{1}{2}] \right\} \tag{50}$$

and noting that the inlet fully-developed velocity profile and vorticity are functions of the channel height (Table 2 yields the upper inlet CSE boundary conditions

$$\begin{Bmatrix} {}^{H}u^f \\ {}^{H}\omega^f \end{Bmatrix} = \frac{D\left\{ u^f \; \omega^f \right\}}{DH_1} - \begin{Bmatrix} \nabla u^f \\ \nabla \omega^f \end{Bmatrix} \cdot \frac{\partial X_{\Gamma_1^{inlet}}}{\partial H_1} = \frac{1}{2\mu} \begin{Bmatrix} -yp_{,x} \\ p_{,x} \end{Bmatrix} - \begin{Bmatrix} -2yu^f_{,y} \\ -2y\omega^f_{,y} \end{Bmatrix} \tag{51}$$

The upper outlet boundary conditions are handled in the same manner, however the y-component gradient of both v^f and p^f are zero and the uniform outflow does not change, so the outlet boundary conditions reduce to zero. No other boundaries are affected by a variation in upper channel height and thus the remaining CSE boundary conditions are homogenous.

The least-squares CSE solution is given in Figure 5 and the beam deflection is compared to approximate-analytic sensitivity [48] in Figure 6 . The approximate-analytic sensitivity is determined by a pseudo-pressure transverse load on the beam. The pseudo-pressure load on beam is the differential pressure change in a channel of constant flow rate due to a variation in channel height. The maximum difference between the CSE and approximate-analytic results is less than 10%. Note that a p-value of 12 (an order of magnitude higher) was needed for an equivalent residual level of the original FSI system. Examining the element residual plot in Figure 5 , however, it is clear that the mesh is far from optimally graded. Nevertheless, the need for a more refined solution to the CSE equations is an observation previously made with regard to other systems [15]. It is convenient to use the same mesh for both the original system and the sensitivity system. This is a distinct advantage of higher-order FEM since p-refinement allows a straightforward means to achieve a refined solution without needing a refined mesh.

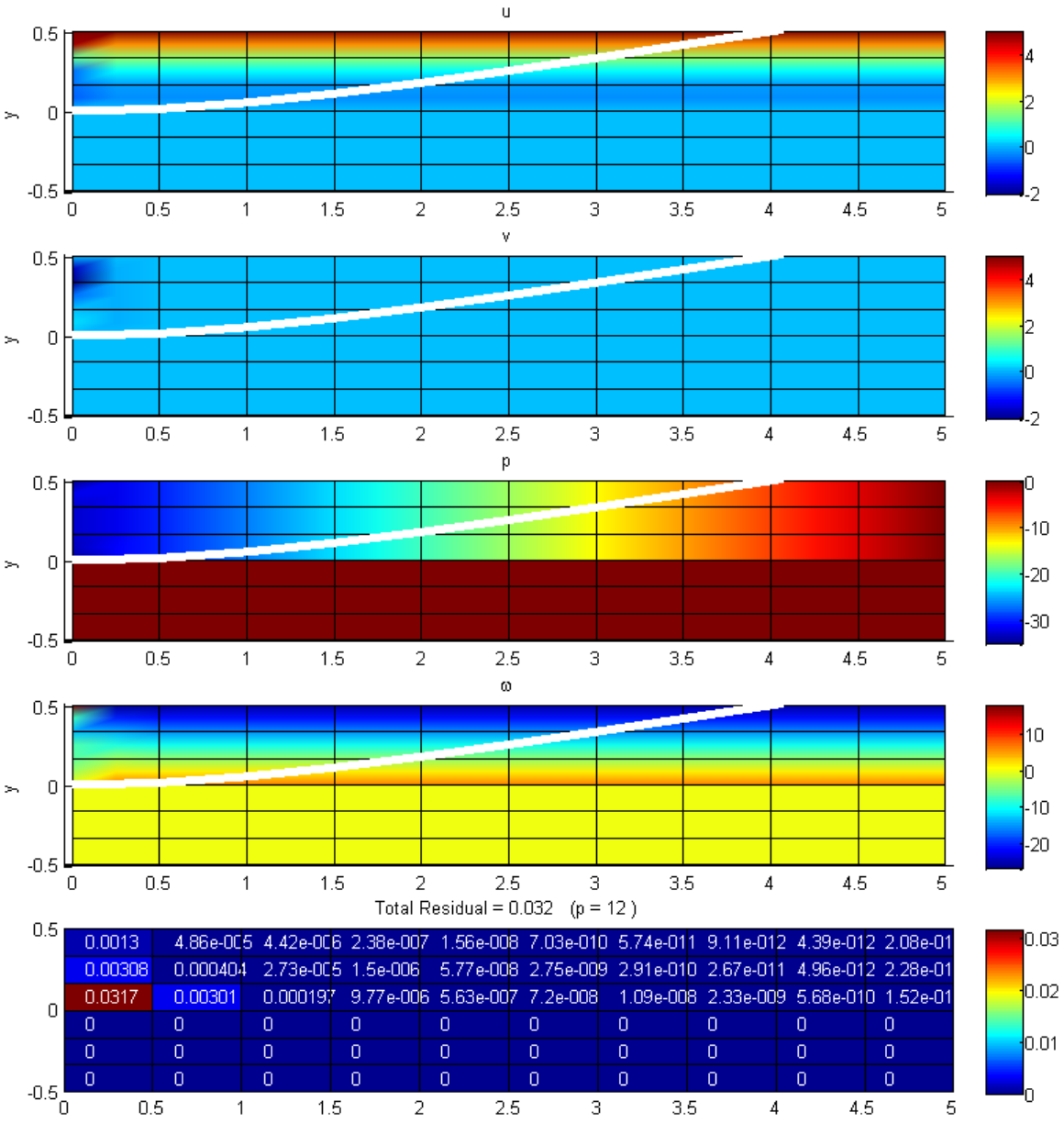

Figure 5 LS CSE solution (p = 12) showing beam deflection sensitivity

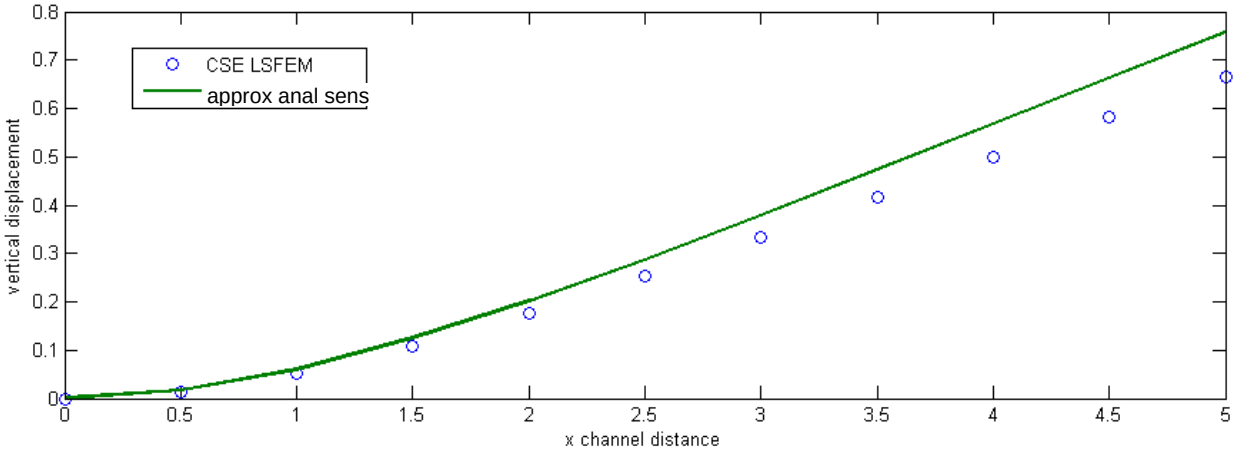

Figure 6 LSFEM CSE beam deflection sensitivity

VI. Conclusion

A least-squares continuous sensitivity analysis method was developed for fluid-structure interaction problems. LSFEM was used to solve both the monolithic, fully-coupled system and the continuous sensitivity system. Gradients of the LSFEM solution and boundary conditions permitted a straightforward method for specifying the CSE boundary conditions. An example fluid-structure interaction problem was solved and the results were compared to the analytic solution and approximate-analytic sensitivity. The CSE equations required a higher *p*-value for equivalent residual error, a result previously observed. The higher-order least-square method employed permitted a straightforward method for CSE solution refinement on the same original computational mesh. Overall, the least-squares, continuous sensitivity analysis approach appears promising and should be applicable to more complicated, transient, nonlinear fluid-structure interaction problems.

VII. Acknowledgements

The Air Force Research Laboratory (AFRL) Air Vehicles Directorate funded this research. The authors gratefully acknowledge the support of the AFRL Senior Aerospace Engineers Dr. Raymond Kolonay, Dr. Phillip Beran, and Dr. Maxwell Blair.

VIII. References

[1] Rasmussen, C., Canfield, R., and and Reddy, J.N., "Nonlinear Transient Gust Response Using a Fully- Coupled Least-Squares Finite Element Formulation," Vol. AIAA-2008-1821, 2008,

[2] Livne, E., "Future of Airplane Aeroelasticity," *Journal of Aircraft,* Vol. 40, No. 6, 2003, pp. 1066--1092.

[3] Bendiksen, O.O., "Modern developments in computational aeroelasticity," *Journal of Aerospace Engineering,* Vol. 218, 2004, pp. 157.

[4] Hubner, B., Walhorn, E., and Dinkler, D., "A monolithic approach to fluid–structure interaction using space–time finite elements," *Computer Methods in Applied Mechanics and Engineering,* 2004,

[5] Etienne,S. (Ecole Polytechnique de Montreal), "A monolithic formulation for unsteady Fluid-structure Interactions," *Collection of Technical Papers - 44th AIAA Aerospace Sciences Meeting, Collection of Technical Papers - 44th AIAA Aerospace Sciences Meeting,* Vol. 11, 2006, pp. 8301.

[6] Walhorn, E., Kölke, A., Hübner, B., "*Fluid-structure coupling within a monolithic model involving free surface flows*," *Computers and Structures,* Vol. 83, 2005, pp. 2100-2111.

[7] Heys, J.J., Manteuffel, T.A., McCormick, S.F., "First-order system least squares (FOSLS) for coupled fluid-elastic problems," *Journal of Computational Physics,* Vol. 195, No. 2, 2004, pp. 560-575.

[8] Bathe, K., and zhang, h., "Finite element developments for general fluid flows with structural interactions," *International Journal for Numerical Methods in Engineering,* Vol. 60, 2004, pp. 213-213-232.

[9] Bathe, K., and Shanhong, H.Z., "Finite element analysis of fluid flows fully coupled with structural interactions," *Computer and Structures,* Vol. 72, 1999, pp. 1-1-16.

[10] Haug, E.J., Choi, K.K., and Komkov, V., "Design sensitivity analysis of structural systems," *Mathematics in science and engineering,* Vol. 177, Academic Press, Orlando, 1986, pp. 381.

[11] Choi, K.K., and Kim, N.H., "Structural sensitivity analysis and optimization," *Mechanical engineering series,* Springer Science+Business Media, New York, 2005,
[12] Borggaard, J., and Burns, J., "A Sensitivity Equation Approach to Shape Optimization in FLuid Flows," Langley Research Center, NASA Contractor Report 191598 (ICASE Report No. 94-8), 1994.
[13] Borggaard, J., and Burns, J., "A PDE Sensitivity Equation Method for Optimal Aerodynamic Design," *Journal of Computational Physics,* Vol. 136, 1997, pp. 366--384.
[14] Haftka, R.T., and Gürdal, Z., "Elements of structural optimization," *Solid mechanics and its applications,* Vol. 11, Kluwer Academic Publishers, Dordrecht ; Boston, 1992, pp. 481.
[15] Stanley, L.G.D., and Stewart, D.L., "Design sensitivity analysis : computational issues of sensitivity equation methods," *Frontiers in applied mathematics,* Society for Industrial and Applied Mathematics, Philadelphia, 2002, pp. 139.
[16] Dems, K., and Haftka, R.T., "Two Approaches to Sensitivity Analysis for Shape Variation of Structures," *Mech. Struct. & Mach.,* Vol. 16, No. 4, 1988-1989, pp. 501-501-522.
[17] Arora, J.S., Lee, T.H., and Cardoso, J.B., "Structural Shape Design Sensitivity Analysis: A Unified Viewpoint," *AIAA-91-1214-CP,* 1991, pp. 675-675-683.
[18] Lund,E. (Institute of Mechanical Engineering, Aalborg University), "Shape design optimization of steady fluid-structure interaction problems with large displacements," *Collection of Technical Papers - AIAA/ASME/ASCE/AHS/ASC Structures, Structural Dynamics and Materials Conference,* Vol. 5, 2001, pp. 3241.
[19] Etienne, S., Hay, A., Garon, A., "Shape Sensitivity Analysis of Fluid-Structure Interaction Problems," AIAA, 2006,
[20] Etienne, S., Hay, A., Garon, A., "Sensitivity Analysis of Unsteady Fluid-Structure Interaction Problems," AIAA, 2007,
[21] Newsome, R.W., Berkooz, G., and Bhaskaran, R., "Use of Analytic Flow Sensitivities in Static Aeroelasticity," *AIAA Journal,* Vol. 36, No. 8, 1998, pp. 1537-1537-1540.
[22] Kayser-Herold, O., and Matthies, H.G., "A Unified Least-Squares Formulation for Fluid-Structure Interaction Problems," *Computer and Structures,* Vol. 85, 2007, pp. 998-998-1011.
[23] Rasmussen, C.C., Canfield, R.A., and Reddy, J.N., "The Least-Squares Finite Element Method Applied to Fluid-Structure Interaction Problems," AIAA, 2007.
[24] Bochev, P.B., and Gunzburger, M.D., "Finite Element Methods of Least-Squares Type," *SIAM Review,* Vol. 40, No. 4, 1998, pp. 789--837.
[25] Jiang, B., "The least-squares finite element method : theory and applications in computational fluid dynamics and electromagnetics," *Scientific computation,* Springer, Berlin ; New York, 1998, pp. 418.
[26] Yang, S., and Liu, J., "Analysis of Least Squares Finite Element Methods for A Parameter-Dependent First-Order System," *Numerical Functional Analysis and Optimization,* Vol. 19, 1998, pp. 191-213.
[27] Bramble, J.H., Lazarov, R.D., and Pasciak, J.E., " Least-squares methods for linear elasticity based on a discrete minus one inner product." *Comput. Methods Appl. Mech. Engrg.,* Vol. 152, 2001, pp. 520--543.
[28] Proot, M. M. J., "The least-squares spectral element method: theory, implementation and application to incompressible flows," 2003,
[29] Cai, Z., Manteuffel, T., McCormick, S., " *First-order system least squares for the Stokes equations, with application to linear elasticity*," *SIAM Journal of Numerical Analysis,* Vol. 34, No. 5, 1997, pp. 1727--1741.
[30] Pontaza, J.P., "Least-squares variational principles and the finite element method: theory, formulations, and models for solid and fluid mechanics," *Finite Elements in Analysis and Design,* Vol. 41, No. 7-8, 2005, pp. 703.
[31] Pontaza, J.P., "Least-squares finite element formulation for shear-deformable shells," *Computer Methods in Applied Mechanics and Engineering,* Vol. 194, No. 21-24, 2005, pp. 2464.
[32] Kayser-Herold, O., and Matthies, H.G., "Least-Squares FEM Literature Review," Institute of Scientific Computing Technical University Braunschweig, 2005-05, Brunswick, Germany, 2005.
[33] Blair, M., Canfield, R.A., and Roberts, R., "A Joined-Wing Aeroelastic Design with Geometric Non-Linearity," *Journal of Aircraft,* Vol. 42, No. 4, 2005, pp. 832-832–848.
[34] Demasi, L., and Livne, E., "Exploratory Studies of Joined Wing Aeroelasticity," AIAA, 2005,
[35] Lee, S.-, Youn, S.-, Yeon, J.-, "A Study on the Fluid-Structure Interaction using LSFEM," Dep. of Mechanical Engineering, Korea Advanced Institute of Science and Technology, Taejon, Korea, 2000.
[36] Kayser-Herold, O., "Least-Squares Methods for the Solution of Fluid-Structure Interaction Problems," 2006,
[37] White, F.M., "Viscous fluid flow," *McGraw-Hill series in mechanical engineering,* McGraw-Hill, New York, 1991, pp. 614.
[38] Hodges, D.H., and Pierce, G.A., "Introduction to structural dynamics and aeroelasticity," *Cambridge aerospace series,* Vol. 15, Cambridge University Press, Cambridge, England ; New York, 2002, pp. 170.
[39] Sackinger, P.A., Schunk, P.R., and Rao, R.R., "A Newton–Raphson Pseudo-Solid Domain Mapping Technique for Free and Moving Boundary Problems: A Finite Element Implementation," *Journal of Computational Physics,* Vol. 125, No. 1, 1996, pp. 83-83-103.
[40] Gel□fand, I.M., Fomin, S.V., and Silverman, R.A., "Calculus of variations," Dover Publications, Mineola, N.Y., 2000, pp. 232.
[41] Reddy, J.N., "An introduction to the finite element method," *McGraw-Hill series in mechanical engineering,* McGraw-Hill Higher Education, New York, NY, 2006, pp. 766.

[42] Naylor, A.W., and Sell, G.R., "Linear operator theory in engineering and science," *Applied mathematical sciences,* Vol. 40, Springer-Verlag, New York, 1982, pp. 624.
[43] Cook, R.D., Malkus, D.S., and Plesha, M.E., "Concepts and applications of finite element analysis," Wiley, New York, 1989, pp. 630.
[44] Šolin, P., Segeth, K., and Doležel, I., "Higher-order finite element methods," *Studies in advanced mathematics,* Chapman & Hall/CRC, Boca Raton, FL, 2004, pp. 382.
[45] Szabo, B.A., and Babuška, I., "Finite element analysis," Wiley, New York, 1991, pp. 368.
[46] Karniadakis, G., and Sherwin, S.J., "Spectralhp element methods for computational fluid dynamics," *Numerical mathematics and scientific computation,* Oxford University Press, New York, 2005, pp. 657.
[47] Wickert, D.P., Canfield, R.A., and Reddy, J.N., "Continuous Sensitivity Analysis Methods of Transient Fluid-Structure Interaction Problems using Least-Squares Finite Elements," to be published.
[48] Wang, X., "Analytical and computational approaches for some fluid-structure interaction analyses," *Computers and Structures,* Vol. 72, 1999, pp. 423-423-433.